Electronic Supplementary Material (ESI) for Nanoscale.

Adsorption on alumina nanopores with conical shape

Lorenzo Bruschi,[a] Giampaolo Mistura,[a,] Fabrizia Negri[b], Benoit Coasne [c,*] Yashar Mayamei[d] and Woo Lee[d,e*]*

[a] Dipartimento di Fisica e Astronomia G. Galilei, Università di Padova, via Marzolo 8, 35131 Padova (Italy)

[b] Dipartimento di Chimica G. Ciamician, Università di Bologna, via Selmi 2, 40126 Bologna and INSTM UdR Bologna (Italy)

[c] Univ. Grenoble Alpes, CNRS, LIPhy, 38000 Grenoble (France)

[d] Department of Nano Science, University of Science and Technology (UST), Yuseong, Daejeon 34113 (Korea)

[e] Korea Research Institute of Standards and Science (KRISS), Yuseong, Daejeon 34113 (Korea)

CORRESPONDING AUTHORS: To whom correspondence should be addressed.

Prof. G. Mistura: giampaolo.mistura@unipd.it

Dr. B. Coasne: benoit.coasne@univ-grenoble-alpes.fr

Dr. W. Lee: woolee@kriss.re.kr

S1. Discontinuous anodizing method

One side of mirror finished aluminum disks (2 cm in diameter, Goodfellow, 99.999 %) is first anodized in 0.3 M $H_2C_2O_4$ (1 ^oC) at 40 V for 24 h. Then, the samples are immersed into an aqueous mixture of 1.8 wt% CrO_3 and 6 wt% H_3PO_4 to remove oxide layer with disordered pores, which results in aluminum disks textured with ordered arrays of approximately hemispherical concavities. Each concavity on the surface of the aluminum acts as a pore initiation site during the subsequent DA process. The DA is performed at 15 ^oC in an aqueous mixture solution comprised of 0.3 M $H_2C_2O_4$ and 0.0087 M H_3PO_4 by applying potential pulses at 40 V (duration = 10 min) separated each other by a 20 min of relaxation period at 0 V. During the relaxation period, pore wall oxide of the previously grown AAO undergoes acidic dissolution by anodizing electrolyte. Since the degree of pore wall dissolution is proportional to the time exposed to the acid electrolyte, the pore diameter decreases progressively from the top to bottom without any sharp transition as confirmed by our scanning electron microscopy (SEM) analysis. Under the present DA condition, the rate of pore wall dissolution turns out to be about 0.88 $nm \cdot h^{-1}$. The bottom end of the resulting as-anodized AAO with conical pores is closed with a thin barrier oxide layer that is in contact with the underlying aluminum substrate. AAO with conical pores open at both ends are obtained by performing selective removal of the aluminum substrate, followed by opening of the barrier layer, as described in Ref. [S1] (see also section S3).

Figure S1 shows two low-resolution SEM images of the top and bottom faces of the same sample analyzed in Fig. 1, together with two histograms of the pore size distribution deduced from micrographs of the two ends, which present sharp, monomodal distributions.

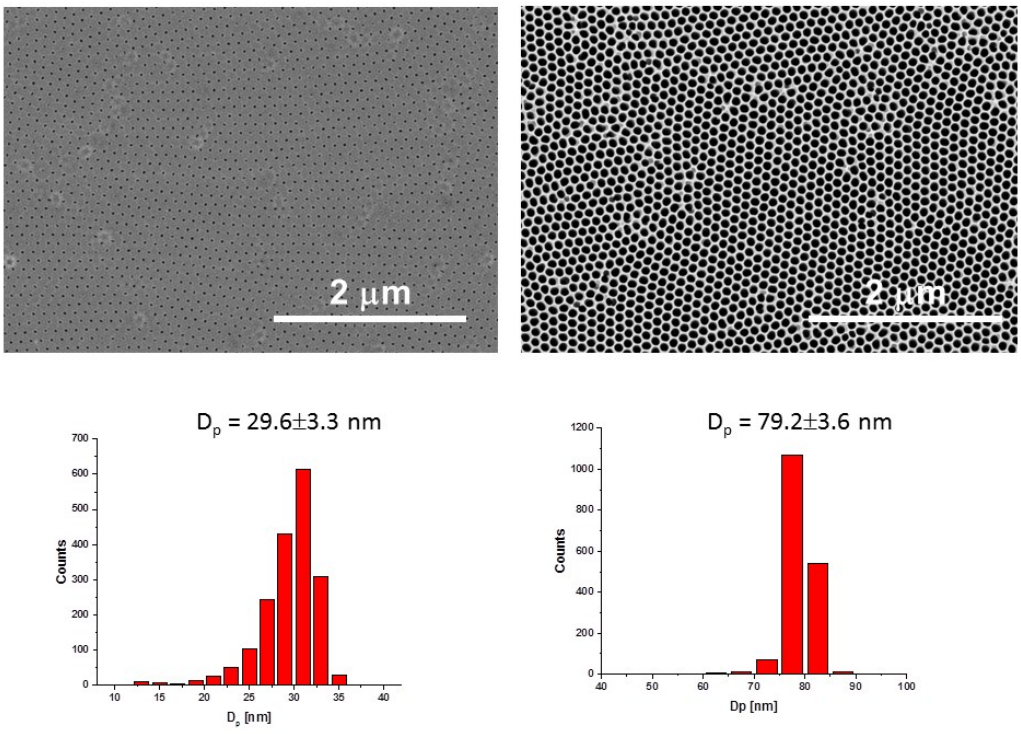

Fig. S1. Top: Plane-view SEM micrographs obtained from the two opposite faces presenting the narrow and wide openings. Bottom: calculated histograms presenting the size distributions of the narrow and wide pore openings.

S2. Surface chemistry of the AAO pore walls

The surface of the AAO pores is terminated with hydroxide (-OH) group, see Ref. [S2]. The surface charge of a properly dried AAO should be neutral, which is the case of our Ar adsorption study. On the other hand, the surface can be charged in an electrolyte solution. The pore wall surface of AAO exhibits amphoteric behavior with surface charge properties that are determined by the solution pH. The isoelectric point of the pore wall surface of AAO formed by oxalic acid anodization is pH 6.5, see Ref. [S3]. Thus, below pH 6.5, AAO is protonated and has positively charged surface: $Al–OH + H^+ \rightarrow Al–OH_2^+$. On the other hand, the surface of AAO is negatively charged in solution pH above 6.5 due to the deprotonation: $Al–OH + OH^- \rightarrow Al–O^- + H_2O$. Accordingly, the surface charge density should be dependent on the solution pH. In order to explain their experimentally observed ion current rectification (ICR) characteristics of porous AAO, Li et al. have employed surface charge density varying from +20 mC/m^2 (in low pH) to -20 mC/m^2 (in high pH) in finite element method (FEM) simulation based on Poisson-Nernst-Planck equation, see Ref. [S4].

S3. Sample fabrication process

As we mentioned in the main text, the sample 1 (Open 1 in Figure 2) adsorbs about three times more than sample 2 (Open 2 in Figure 2) due to the larger patterned area. Two samples were prepared at the same anodizing batch. After anodization, through-hole AAO membranes were prepared by selective removal of the underlying Al substrate, followed by opening of the barrier layer (see Fig. S2). For the removal of the Al substrate, the central region of the backside of the anodized samples was selectively exposed to the aluminum etching solution, which could be achieved by placing the sample in an electrochemical cell with an O-ring (typical diameter = 1.0 cm). However, the opening (d) in Fig. S2 (b) after the selective Al etching varied from sample to sample, depending on the Al etching time, which influences "The patterned area" in the main text.

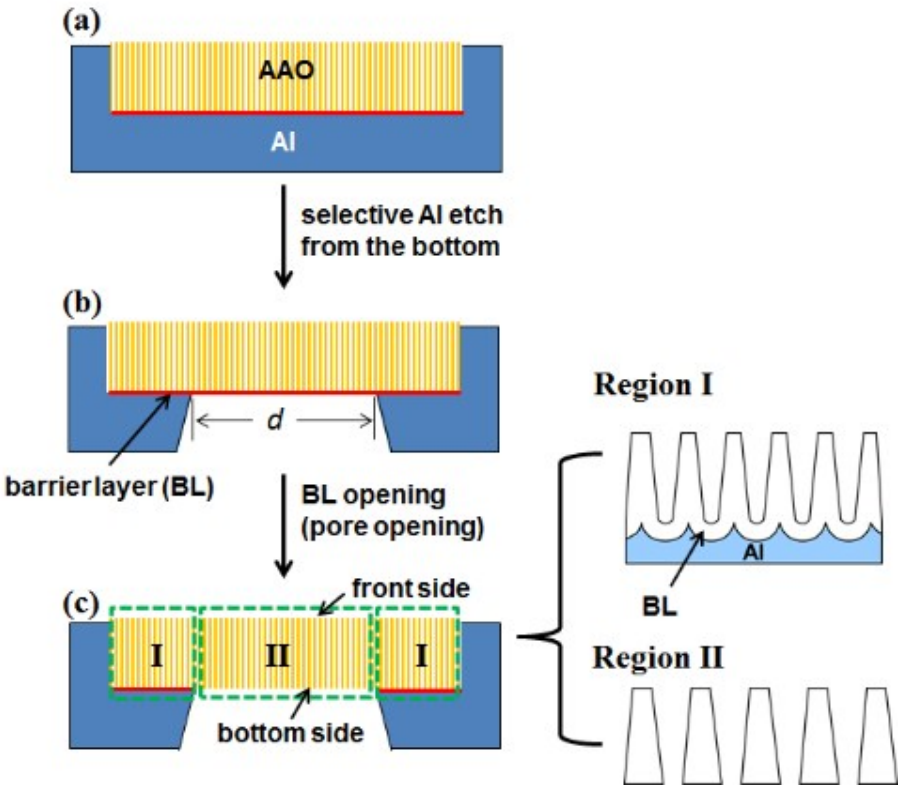

Fig. S2. Schematic procedure of preparation of funnel-shaped AAO membrane: (a) as-prepared AAO, (b) after selective backside etching of Al substrate, and (c) after removal of barrier layer (BL). Regions I and II refer respectively to the outer ring comprised of closed bottom pores and the central area with open bottom pores. For the detailed description of the process, see Ref. [S5].

S4. On-lattice Grand Canonical Monte Carlo

On-lattice Grand Canonical Monte Carlo simulations is a stochastic method that simulates a fluid lattice having a constant volume V (the pore with the adsorbed phase) in equilibrium with an infinite reservoir of particles imposing a chemical potential μ and temperature T. The absolute adsorption isotherm

corresponds to the ensemble average of the number of adsorbed particles as a function of the pressure of the gas reservoir P (the latter is assumed to correspond to the fugacity which is readily obtained from the chemical potential μ). Periodic boundary conditions are used along the 3 directions x, y, z to avoid finite size effects.

The critical temperature is assessed by determining the density-chemical potential phase diagram for the bulk fluid at different reduced temperatures T^* (Fig. ~~S1~~S3). At low temperature, i.e. below the bulk critical point T_c, the density as a function of the chemical potential exhibits a discontinuous, irreversible transition upon increasing the chemical potential; the fluid undergoes a first order phase transition between a low density phase (gas) to a high density phase (liquid). In contrast, above the critical temperature T_c, the transition between the low and high density phases occurs in continuous and reversible fashion as the transition becomes second order. T_c is therefore determined as the temperature at which the transition switches from discontinuous to continuous.

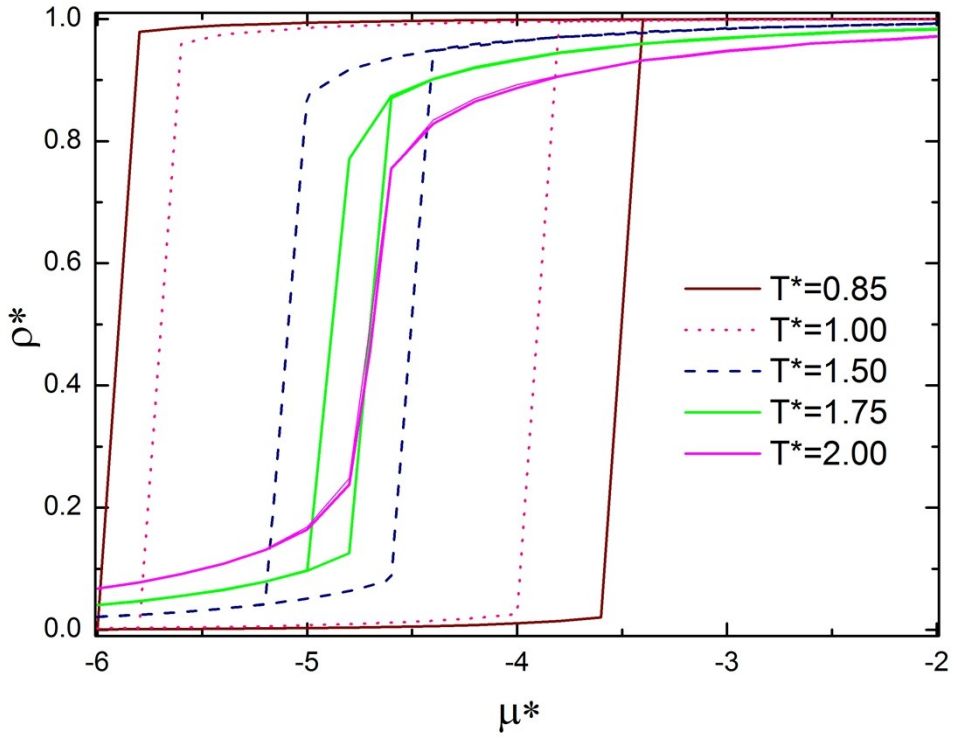

Fig. S3. Density-chemical potential phase diagram for the bulk lattice fluid at different temperatures. Note the large hysteresis loop for the data below the critical point T* ~ 2. The asterisk * indicates reduced quantities with respect to the energy parameter ε and lattice spacing σ.

References

S1. L. Bruschi, G. Mistura, P. T. M. Nguyen, D. D. Do, D. Nicholson, S.-J. Park, and W. Lee, *Nanoscale,* 2015, **7**, 2587-2596.

S2. W. Lee and S.-J. Park, *Chem. Rev*., 2014, **114**, 7487-7556.

S3. W. Chen, J.-H. Yuan, X.-H. Xia, *Anal. Chem.,* 2005, **77**, 8102-8108.

S4. C.-Y. Li, F.-X. Ma, Z.-Q. Wu, H.-Li Gao, W.-T. Shao, K. Wang, X.-H. Xia, *Adv. Funct. Mater.,* 2013, **23**, 3836-3844.

S5. L. Bruschi, G. Mistura, S.-J. Park, W. Lee, *Adsorption* 2014, **20**, 889–897.